

Early Spectral Evolution of the Rapidly Expanding Type Ia SN 2006X

Masayuki YAMANAKA^{1,2,3}, Hiroyuki NAITO⁴, Kenzo KINUGASA⁵, Naohiro TAKANASHI⁶,
Masaomi TANAKA⁷, Koji S. KAWABATA², Shinobu OZAKI⁸, Shin-ya NARUSAWA⁴,
and Kozo SADAKANE³,

¹*Department of Physical Science, Hiroshima University, Kagamiyama 1-3-1, Higashi-Hiroshima
739-8526*

²*Hiroshima Astrophysical Science Center, Hiroshima University, Higashi-Hiroshima, Hiroshima
739-8526*

³*Astronomical Institute, Osaka Kyoiku University, Asahigaoka, Kashiwara-shi, Osaka 582-8582*

⁴*Nishi-Harima Astronomical Observatory, Sayo-cho, Hyogo, 679-5313*

⁵*Gunma Astronomical Observatory, Takayama, Gunma 377-0702*

⁶*National Astronomical Observatory of Japan, Mitaka 181-8588*

⁷*Department of Astronomy, School of Science, University of Tokyo, Bunkyo-ku, Tokyo 113-0033*

⁸*Okayama Astrophysical Observatory, National Astronomical Observatory of Japan, Kamogata,
Asakuchi-shi, Okayama 719-0232
myamanaka@hiroshima-u.ac.jp*

(Received 2008 August 17; accepted 2009 April 13)

Abstract

We present optical spectroscopic and photometric observations of Type Ia supernova (SN) 2006X from -10 to $+91$ days after the B -band maximum. This SN exhibits one of the highest expansion velocity ever published for SNe Ia. At premaximum phases, the spectra show strong and broad features of intermediate-mass elements such as Si, S, Ca, and Mg, while the O I $\lambda 7773$ line is weak. The extremely high velocities of Si II and S II lines and the weak O I line suggest that an intense nucleosynthesis might take place in the outer layers, favoring a delayed detonation model. Interestingly, Si II $\lambda 5972$ feature is quite shallow, resulting in an unusually low depth ratio of Si II $\lambda 5972$ to $\lambda 6355$, $\mathcal{R}(\text{Si II})$. The low $\mathcal{R}(\text{Si II})$ is usually interpreted as a high photospheric temperature. However, the weak Si III $\lambda 4560$ line suggests a low temperature, in contradiction to the low $\mathcal{R}(\text{Si II})$. This could imply that the Si II $\lambda 5972$ line might be contaminated by underlying emission. We propose that $\mathcal{R}(\text{Si II})$ may not be a good temperature indicator for rapidly expanding SNe Ia at premaximum phases.

Key words: Spectroscopy — Star: supernovae — Supernovae: individual:

1. Introduction

Type Ia supernovae (SNe Ia) are thermonuclear explosions of C+O white dwarfs. It is thought that the explosion is triggered when the mass of the white dwarf approaches the Chandrasekhar limit ($\sim 1.4M_{\odot}$). Their peak luminosity, calibrated using the correlation with the light curves and/or color curves, is quite uniform, and thus, SNe Ia have been used as “standard candles” for measuring the extragalactic distances (Phillips 1993; Phillips et al. 1999; Wang et al. 2005). Observations of distant SNe Ia led to the discovery of the accelerating expansion of the universe (Riess et al. 1998; Perlmutter et al. 1999).

Spectroscopic properties and their time evolution had been thought to be homogeneous in SNe Ia (e.g., Branch et al. 1993; Filippenko 1997). However, recent spectroscopic observations show that the spectra of SNe Ia at premaximum phases show diversity in their line velocities and profiles (Fisher et al. 1997; Benetti et al. 2004; Mazzali et al. 2005a; Mazzali et al. 2005b; Quimby et al. 2006b; Altavilla et al. 2007; Garavini et al. 2007; Phillips et al. 2007; Sahu et al. 2008; Wang et al. 2009). In particular, the Doppler velocity of Si II $\lambda 6355$ feature exhibits a large dispersion, and the velocity is not correlated with the peak luminosity (Hatano et al. 2000).

Benetti et al. (2005) collected some well-observed SNe Ia sample and divided them into three groups according to the luminosity and the temporal gradient of the Si II velocity. SNe Ia with both high velocity gradient (HVG) and low velocity gradient (LVG) have normal luminosity, while the FAINT group is dimmer than the two classes above, as represented by subluminal SN Ia 1991bg (Filippenko et al. 1992). Branch et al. (2006) studied near-maximum spectra of SNe Ia and defined four groups according to the equivalent width ratio of Si II $\lambda 6355$ and Si II $\lambda 5972$ and also the profile of the Si II $\lambda 6355$ line near the maximum light. These studies show that the physics of SNe Ia cannot be represented by a family of one parameter such as the luminosity decline rate $\Delta m_{15}(B)$ ¹ (Benetti et al. 2004).

Nugent et al. (1995) found that the depth ratio of Si II $\lambda 5972$ to Si II $\lambda 6355$, $\mathcal{R}(\text{Si II})$, is correlated with the absolute luminosity of SNe Ia at maximum brightness. It is thought that $\mathcal{R}(\text{Si II})$ is an indicator of the temperature of the photosphere. At the premaximum phases, $\mathcal{R}(\text{Si II})$ shows considerable diversity. Benetti et al. (2005) showed that, at the premaximum phases, $\mathcal{R}(\text{Si II})$ in HVG SNe is high in the earliest phases and declines rapidly, while that of LVG SNe does not change significantly. Tanaka et al. (2008) suggested that the photospheric temperature in HVG SNe is lower than that of LVG SNe at premaximum phases ($\gtrsim 1$ week before maximum) from their spectrum analysis.

¹ The difference between the B -band magnitudes at maximum and that at 15 days after the maximum (Phillips 1993).

SN 2006X ($\alpha_{2000} = 12^h 22^m 53^s.90$, $\delta_{2000} = -15^\circ 48' 32.9''$) was discovered on 2006 February 4.75 UT by S. Suzuki and M. Migliardi (2006), independently, near the center of the nearby galaxy NGC 4321 (M100). The distance to NGC 4321 is derived as $\mu = 30.91 \pm 0.14$ by the Cepheid calibration of the Hubble Space Telescope Key Project (Freedman et al. 2001). Quimby et al. (2006a) classified SN 2006X as Type Ia. They reported that the Si II $\lambda 6355$ line velocity of this SN was very high ($20,700 \text{ km s}^{-1}$) on February 8.35 ($t = -11.6$ d, hereafter, t denotes days from the B -band maximum, MJD=53785.67. See §2.1.). Wang et al. (2008a) presented extensive optical and NIR photometric observations. They derived maximum absolute magnitude $M_{V,\text{max}} = -19.06 \pm 0.17$, decline rate of the B -band light curve $\Delta m_{15}(B) = 1.17 \pm 0.05$, and maximum bolometric luminosity $L_{\text{bol,max}} \simeq 1.0 \times 10^{43} \text{ erg s}^{-1}$, suggesting that this SN is a normally luminous SN Ia. Wang et al. (2008a) obtained spectra around and after the maximum, and suggested that SN 2006X is characterized by strong, highly blueshifted absorption lines of intermediate-mass elements. The Si II $\lambda 6355$ absorption is very deep and broad at one week after the maximum, similar to that in SNe 1984A and 2002bo (Branch et al. 2008). Patat et al. (2007) reported the detection of the temporal variation of Na I D absorption line and suggested the presence of dense circumstellar materials (CSM) around SN 2006X. The possible detection of an inner echo might be also consistent with the circumstellar dust scenario (Wang et al. 2008b).

In this paper, we present spectroscopic and photometric observations of SN 2006X. In particular, we show optical spectra at premaximum phases, which are not presented by Wang et al. (2008a). The premaximum spectra are useful to explore the physical properties in the outermost layers of the SN ejecta. Our observations and data reduction are described in §2. Results are shown in §3. We discuss the spectroscopic properties of SN 2006X at the premaximum phases in §4, and finally give conclusions in §5.

2. Observations and Data Reduction

2.1. Photometric Observations

We performed BVR_cI_c photometric observations on 24 nights from $t = -10$ d to $+91$ d with two telescopes; a 0.6m reflector equipped with an ST-9 imager at Nishi-Harima Astronomical Observatory (NHAO) and a 0.51m telescope equipped with a CCD camera at Osaka Kyoiku University (OKU). Data reduction was performed in a standard manner for aperture photometry using *IRAF*². Although there is a star located at $1''$ east and $8''$ north

² *IRAF* is distributed by the National Optical Astronomy Observatories, operated by the Association of Universities for Research in Astronomy, Inc., under contract to the National Science Foundation of the

of the SN, it is faint ($V=17.05$, Wang et al. 2008a), thus our photometry is not significantly affected by this star except for the measurements at the last two epochs. We performed the PSF photometry for the last two-epoch images, and derived the magnitudes that are consistent with those in Wang et al. (2008a), within 2σ error. The photometric calibration was performed using the comparison stars in Wang et al. (2008a). A summary of our photometric observations is shown in table 1.

From our data, we derived the date of B -band maximum at $\text{MJD} = 53785.1 \pm 1.8$ and maximum magnitude $m_{B,max} = 15.30 \pm 0.09$ by a polynomial fitting. Both are consistent with those in Wang et al. (2008a), who derived the B -band maximum date and magnitude as 53785.67 ± 0.35 and 15.40 ± 0.03 , respectively. In this paper, we assume $\text{MJD} = 53785.67$ as $t = 0$ d for the convenience of comparison with their study.

2.2. Spectroscopic Observations

Spectroscopic observations were performed on 22 nights from $t = -10$ d to $+84$ d. 18 spectra were taken at NHAO, including four at premaximum phases, with the 2m NAYUTA telescope and a low-resolution spectrograph, MALLS (Medium And Low-dispersion Long-slit Spectrograph; Ozaki & Tokimasa 2005). The typical exposure time is 1800 s. The wavelength coverage is 4000–6800 Å and the wavelength resolution is ~ 17 Å, corresponding to a velocity resolution of 850 km s^{-1} at 6000 Å. Four spectra were taken at Gunma Astronomical Observatory (GAO), including two at premaximum phases, with the 1.5m telescope equipped with a low-resolution spectrograph, GLOWS (Gunma LOW resolution Spectrograph and imager). The wavelength coverage is 4000–8000 Å and the wavelength resolution is ~ 15 Å (750 km s^{-1}). One late-time spectrum (at $t = 63$ d) was obtained by using the 8.2 m Subaru Telescope (National Astronomical Observatory of Japan) and FOCAS (Faint Object Camera And Spectrograph; Kashikawa et al. 2002), with the wavelength coverage being 4000–9000 Å and the wavelength resolution being ~ 14 Å (700 km s^{-1}). The log of our spectroscopic observations is shown in table 2.

Data reduction was performed by the standard procedure for long-slit spectroscopy with *IRAF* tasks. Sky background was subtracted by 1D interpolation along the focal slit direction. The wavelength calibration was obtained by using night-sky lines taken in the object frames (for NHAO data; Iye et al. 1991) or comparison lamp data (for the others). The flux was calibrated with the data of spectrophotometric standard stars obtained on the same night.

In determining the central wavelength of absorption lines, we used the method described in Hachinger et al. (2006). We first estimated the center of each feature by eyes. Then, we performed 1D Gaussian fitting to the feature several times, and derived the mean central wavelength and its standard deviation. The final uncertainty of the center wavelength was taken as the root sum square of the standard deviation and the wavelength resolution described

above.

3. Results

3.1. Light Curves and Color Curves

We present light curves and color curves in figures 1 and 2, respectively. The light curves are compared with that of SN 1994D (thin lines, Patat et al. 1996). From our data, the light curve decline parameter is derived as $\Delta m_{15}(B) = 1.2 \pm 0.1$, which is consistent with $\Delta m_{15}(B) = 1.17 \pm 0.05$ derived by Wang et al. (2008a). This value is typical for a normal SN Ia (e.g., Phillips et al. 1999).

We derived color excesses as $E(B - V) = 1.26 \pm 0.17$, $E(V - R) = 0.64 \pm 0.13$, and $E(V - I) = 1.23 \pm 0.26$ using the template color indices given by Nobili et al. (2008). These values are also consistent with those by Wang et al. (2008a) within 1σ error. In figure 2, $B - V$, $V - R$ and $V - I$ curves are compared with those of other SNe Ia, SNe 2002bo (Krisciunas et al. 2004), 2002er (Pignata et al. 2004), 2003cg (Elias-Rosa et al. 2006), and 2003du (Stanishev et al. 2007). The color curves of these SNe are shifted arbitrary to match those of SN 2006X. We find no significant difference between them.

3.2. Spectral Evolution

The complete spectral evolution of SN 2006X spectra from $t = -10$ d to $+84$ d is shown in figure 3. The spectra have been corrected for the redshift of the host galaxy ($v = +1,571$ km s⁻¹; (Rand 1995)). We show spectra at $t = -10$ d and -6 d in figures 4 and 5, respectively, compared with those of other SNe Ia at similar phases³. For the reddening correction, we assumed a color excess of $E(B - V) = 1.42$ and an extinction coefficient of $R_V = A_V/E(B - V) = 1.48$ (Wang et al. 2008a). Line identifications are given by comparison with well-studied SNe Ia 2003cg (Elias-Rosa et al. 2006), 2002er (Kotak et al. 2005), 2002bo (Benetti et al. 2004), and 2003du (Stanishev et al. 2007).

At $t = -10$ d (figure 4), the absorption of the Si II $\lambda 6355$ line has the minimum at 5950 Å, corresponding to an expansion velocity of about 19,000 km s⁻¹. This is one of the highest expansion velocity that has ever been observed for SNe Ia at similar phases. The velocity measured from Si II $\lambda 5972$ is found to be as high as 17,000 km s⁻¹. The W-shaped S II $\lambda 5468$ and S II $\lambda 5640$ (the blend of $\lambda 5612$ and $\lambda 5654$) lines also show larger blueshifts than those of other SNe Ia shown in figure 4. The features around 4700 Å and 4200 Å are also broad, and largely blueshifted. The Si III $\lambda 4560$ line is not strong, which may be common in the fast-expanding SNe Ia (Pignata et al. 2008). In the $t = -9.8$ d GAO spectrum (figure 3), a weak O I $\lambda 7773$ line can be seen around 7300 Å. A broad absorption trough is also seen around 7800 Å. If this trough is produced by the Ca II IR triplet, the expansion velocity reaches $\gtrsim 26,000$

³ We took the spectra from the SUSPECT database;
<http://bruford.nhn.ou.edu/~suspect/index.html>.

km s⁻¹.

At $t = -6$ d (figure 5), the blueshift of the absorption features is still large. The Si II $\lambda 6355$ absorption remains deep and broad. In contrast, the Si II $\lambda 5972$ feature becomes unusually weak. The blueshift of the W-shaped sulfur feature is still larger than those in the comparison SNe Ia. We noticed that the Si III $\lambda 4560$ feature becomes stronger than it appeared at $t = -10$ d (figure 4, see §4.2).

The strong absorption features of intermediate-mass elements such as Si, S, Ca, and Mg maintained throughout the premaximum phases, while the O I $\lambda 7773$ is very weak at $t = -10$ d and almost absent at $t = -1$ d. There is no clear evidence of carbon feature in the spectra of SN 2006X. Implications of these observational properties will be discussed in §4.

The spectral evolution around and after maximum has been studied by Wang et al. (2008a). The line profiles of the spectra between SN 2006X and other SNe Ia in comparison become similar when entering the nebular phase (figure 3). It is noted that the light echo component, which has been found by later phase observations ($t \sim 300$ d) by HST and Keck (Wang et al. 2008b), seems to be negligible during our observational period because there is no excess in the light curve (see figure 2 in Wang et al. 2008b).

4. Discussion

4.1. Extremely Large Expansion Velocity and Constraints on Explosion Model

In figure 6, we present the temporal evolution of the line velocities of Si II $\lambda 6355$ and S II $\lambda 5640$, together with those of other four SNe Ia. It clearly shows that the velocities of SN 2006X are the highest among all the SNe in comparison from premaximum phases to $t = +30$ d. Especially, the Si II $\lambda 6355$ line velocity at $t = -10$ d reaches 19,000 km s⁻¹. For example, the expansion velocity of SN 2006X was found to be higher than that of the normal SNe Ia by $\gtrsim 5000$ km s⁻¹ during the premaximum phase and higher than that of SN 2002bo by 2000-3000 km s⁻¹. Such a high-velocity behavior were also observed in SNe 1983G (Benetti et al. 1991; McCall et al. 1984), 1984A (Barbon et al. 1989), 2002bf (Leonard et al. 2005), 2002bo (Benetti et al. 2004), 2002dj (Pignata et al. 2008), and 2004dt (Altavilla et al. 2007). SN 2006X may be one of them with the highest expansion velocity. The velocity of the S II $\lambda 5640$ lines have also been regarded as a better tracer of the photospheric velocity (Patat et al. 1996). Inspection of figure 6 similarly reveals a photospheric expansion velocity is very high in SN 2006X.

The premaximum spectra can provide constraints on the explosion models. In deflagration models (Nomoto et al. 1984; Röpke et al. 2007), elements heavier than Mg are not synthesized in the outer layers with $v \gtrsim 15,000$ km s⁻¹. In the case of SN 2006X, the Si and S line velocities are higher than 15,000 km s⁻¹, indicating that these intermediate-mass elements are located in such outer layers. Thus, the deflagration models may fail to explain the high velocity lines of intermediate-mass elements in the premaximum spectra.

In delayed detonation models (Khokhlov 1991), an intense nucleosynthesis takes place in the outer layers and the C+O white dwarf is almost completely burned. For example, in the CS15DD2 model in Iwamoto et al. (1999), a Si-rich layer with $X(\text{Si}) \gtrsim 0.1$ extends to $20,000 \text{ km s}^{-1}$. Thus the delayed detonation model may account for the high velocity absorption features of intermediate-mass elements seen in SN 2006X. The weak O I $\lambda 7773$ line is consistent with such a scenario.

Another possible scenario of the increasing apparent line velocity is the interaction of the SN ejecta with the CSM. In SN 2006X, the presence of the CSM around the progenitor has been suggested by Patat et al. (2007) and Wang et al. (2008b). The CSM may be stripped-off atmosphere from the companion star by white dwarf wind during the pre-explosion phase (Hachisu et al. 2008). The interaction between the SN ejecta and the CSM could produce the high velocity Ca II lines (Gerardy et al. 2004) and may also affect the Si II lines (Tanaka et al. 2006). Thus, the CSM interactions could also explain the extremely high Si II and S II line velocities ⁴.

4.2. Line Depth Ratio $\mathcal{R}(\text{Si II})$

We discuss the time evolution of the depth ratio of the two Si lines, $\mathcal{R}(\text{Si II})$. The Si II lines of SN 2006X show unique properties. The Si II $\lambda 6355$ feature was very strong before and around maximum, while the Si II $\lambda 5972$ was visible in the earliest spectra but became subsequently rather weak at around the maximum light. Nugent et al. (1995) defined the depth ratio as

$$\mathcal{R}(\text{Si II}) = \frac{D(\text{Si II} \lambda 5972)}{D(\text{Si II} \lambda 6355)}, \quad (1)$$

where D is the depth of the absorption feature below the pseudo-continuum level. This spectral index is easy to be applied because it does not depend on the reddening correction. The $\mathcal{R}(\text{Si II})$ around the maximum is considered to be an indicator of luminosity and/or temperature for SNe Ia: a SN with lower $\mathcal{R}(\text{Si II})$ is more luminous and shows a higher photospheric temperature (Nugent et al. 1995; Bongard et al. 2006). This is explained by the temperature-sensitive Si II $\lambda 5972$ line, which becomes stronger as the photospheric temperature is lower (Hachinger et al. 2006; Hachinger et al. 2008). The time evolution of the $\mathcal{R}(\text{Si II})$ during the premaximum phases shows diversity among SNe Ia (Benetti et al. 2005). During the premaximum phases, $\mathcal{R}(\text{Si II})$ of HVG SNe decrease while that of LVG SNe stays nearly constant. Around the maximum, the $\mathcal{R}(\text{Si II})$ of HVG and LVG SNe become comparable.

The decline rate of the Si II $\lambda 6355$ line velocity in SN 2006X from $t = 0$ d to +28 d is estimated as $\dot{v} \simeq -130 \text{ km s}^{-1} \text{ day}^{-1}$, which puts this object into the HVG group, similar to

⁴ If the evolution of the Si II and Ca II lines are strongly correlated, CSM interaction scenario may be favored. However, due to the absence of the spectra covering Ca II lines (Ca II H&K or IR triplet lines), we refrain from further discussion.

SNe 2002bo and 2002er (figure 6). In figure 7, we show the time evolution of $\mathcal{R}(\text{Si II})$. The rapidly decreasing trend of $\mathcal{R}(\text{Si II})$ in SN 2006X from $t = -10$ d to -6 d is consistent with SN 2002bo. However, the value of $\mathcal{R}(\text{Si II}) \simeq 0.1$ is unusually low compared to SNe 2002bo and 2002er (although we cannot reject the possibility that $\mathcal{R}(\text{Si II})$ was much higher at earliest epochs, i.e., $t \lesssim -10$ d). The low $\mathcal{R}(\text{Si II})$ is usually interpreted as a high photospheric temperature.

Si III $\lambda 4560$, as another temperature indicator, is expected to be very strong in a SN Ia with high photospheric temperature (Benetti et al. 2004). The Si III $\lambda 4560$ line in HVG SNe Ia is shallower than that of LVG SNe (e.g., Pignata et al. 2008). Tanaka et al. (2008) synthesized spectra for several HVG and LVG SNe Ia at earliest phases ($t \lesssim -1$ week) and suggested that the photospheric temperature of HVG SNe Ia is lower than those of LVG SNe Ia. As shown in figures 4 and 5, the absorption line of Si III $\lambda 4560$ in SN 2006X becomes stronger with time. This fact is consistent with the decreasing trend of $\mathcal{R}(\text{Si II})$. However, the Si III $\lambda 4560$ is as shallow as that of other HVG SNe Ia. This suggests that the photospheric temperature is not very high, being similar to other HVG SNe, which is in contradiction to the low $\mathcal{R}(\text{Si II})$.

We suggest that the $\mathcal{R}(\text{Si II})$ may not be a good temperature indicator for the rapidly expanding SNe Ia at the premaximum phases. It is cautioned that $\mathcal{R}(\text{Si II})$ could be contaminated by other emission components. In fact, Bongard et al. (2008) suggested that the Fe II and Fe III emissions from the inner ejecta form a pseudo-continuum around the Si II $\lambda 5972$ feature, which could weaken the Si II $\lambda 5972$ absorption line. These effects might be strong in the rapidly expanding SNe Ia. To clarify this issue, it is necessary to increase the sample of high-velocity SNe Ia with very early spectroscopic observations.

5. Conclusions

We presented spectroscopic and photometric observations of Type Ia SN 2006X. From our premaximum spectra, it is found that the SN is one of the most rapidly expanding Type Ia SNe. The extremely high velocities of the Si II $\lambda 6355$ and S II $\lambda 5640$ lines and the weakness of O I $\lambda 7773$ line suggest that an intense nucleosynthesis may take place in the outer layers of SN 2006X, consistent with the delayed detonation model. Circumstellar interactions might also explain the high velocity features.

The evolution of the $\mathcal{R}(\text{Si II})$ ratio is unique in SN 2006X. The $\mathcal{R}(\text{Si II})$ is very low throughout the premaximum phases (being unlike the other HVG SNe in comparison), which is usually interpreted as a high temperature. However, the absorption feature of Si III $\lambda 4560$ is as shallow as those in other HVG SNe, suggesting the photospheric temperature is comparable with other HVG SNe. This inconsistency might imply that the Si II $\lambda 5972$ line is weakened by contamination of the underlying emission. We suggest that the $\mathcal{R}(\text{Si II})$ may not be a good temperature indicator for rapidly expanding SNe at premaximum phases.

We would like to thank the NHAO and GAO staff for enabling us to make frequent spectroscopic observations using the NAYUTA telescope and the 1.5-m telescope. The cooperation by graduate students of Osaka Kyoiku University, Y. Ishii, M. Kamada, S. Mizoguchi, S. Nishiyama, N. Sumitomo and K. Tanaka in performing the photometric observations is gratefully acknowledged. We thank an anonymous referee for many comments which helped us in improving this paper. M.T. is supported by the JSPS (Japan Society for the Promotion of Science) Research Fellowship for Young Scientists.

References

- Altavilla, G., et al. 2007, *A&A*, 475, 585
Barbon, R., Iijima, T., & Rosino, L. 1989, *A&A*, 220, 83
Benetti, S., Cappellaro, E., & Turatto, M. 1991, *A&A*, 247, 410
Benetti, S., et al. 2004, *MNRAS*, 348, 261
Benetti, S., et al. 2005, *ApJ*, 623, 1011
Bongard, S., Baron, E., Smadja, G., Branch, D., & Hauschildt, P. H. 2006, *ApJ*, 647, 513
Bongard, S., Baron, E., Smadja, G., Branch, D., & Hauschildt, P. H. 2008, *ApJ*, 687, 456
Branch, D., Fisher, A., & Nugent, P. 1993, *AJ*, 106, 2383
Branch, D., et al. 2006, *PASP*, 118, 560
Branch, D., et al. 2007, *PASP*, 119, 709
Branch, D., et al. 2008, *PASP*, 120, 135
Elias-Rosa, N., et al. 2006, *MNRAS*, 369, 1880
Filippenko, A. V. 1992, *ApJ*, 384, L15
Filippenko, A. V., et al. 1992, *AJ*, 104, 1543
Filippenko, A. V. 1997, *ARA&A*, 35, 309
Fisher, A., Branch, D., Nugent, P., & Baron, E. 1997, *ApJ*, 481, L89
Freedman, W. L., et al. 2001, *ApJ*, 553, 47
Garavini, G., et al. 2007, *A&A*, 471, 527
Gerardy, C. L., et al. 2004, *ApJ*, 607, 391
Hachinger, S., Mazzali, P. A., & Benetti, S. 2006, *MNRAS*, 370, 299
Hachinger, S., Mazzali, P. A., Tanaka, M., Hillebrandt, W., & Benetti, S. 2008, *MNRAS*, 389, 1087
Hachisu, I., Kato, M., & Nomoto, K. 2008, *ApJ*, 679, 1390
Hatano, K., Branch, D., Lentz, E. J., Baron, E., Filippenko, A. V., & Garnavich, P. M. 2000, *ApJ*, 543, L49
Iwamoto, K., Brachwitz, F., Nomoto, K., Kishimoto, N., Umeda, H., Hix, W. R., & Thielemann, F.-K. 1999, *ApJS*, 125, 439
Iye, M., Nishihara, E., & Sugai, H. 1995, *Annual Report of NAOJ*, 295, 423 (in Japanese)

Kashikawa, N., et al. 2002, PASJ, 54, 819
Khokhlov, A. M. 1991, A&A, 245, 114
Kotak, R., et al. 2005, A&A, 436, 1021
Krisciunas, K., et al. 2004, AJ, 128, 3034
Lentz, J. E., Baron, E., Branch, D., & Hauschild, P. H. 2001, ApJ, 547, 402
Leonard, C. D., Li, W., Filippenko, A. V., Foley, R. J., & Chornock, R. 2005, ApJ, 632, 450
Mazzali, P. A., Benetti, S., Stehle, M., Branch, D., Deng, J., Maeda, K., Nomoto, K., & Hamuy, M. 2005a, MNRAS, 357, 200
Mazzali, P. A., et al. 2005b, ApJ, 623, L37
Mazzali, P. A., Röpke, F. K., Benetti, S., & Hillebrandt, W. 2007, Science, 315, 825
McCall, M. L., Reid, N., Bessell, M. S., & Wickramasinghe, D. 1984, MNRAS, 210, 839
Nobili, S., & Goobar, A. 2008, A&A, 487, 19
Nomoto, K., Thielemann, F.-K., & Yokoi, K. 1984, ApJ, 286, 644
Nugent, P., Phillips, M. M., Baron, E., Branch, D., & Hauschildt, P. 1995, ApJ, 455, L147
Ozaki, S., & Tokimasa, N. 2005, Annual Report of NHAO, Vol.,15, 15 (in Japanese)
Patat, F., Benetti, S., Cappellaro, E., Danziger, I. J., della Valle, M., Mazzali, P. A., & Turatto, M. 1996, MNRAS, 278, 111
Patat, F., et al. 2007, Science, 317, 924
Perlmutter, S., et al. 1999, ApJ, 517, 565
Phillips, M. M. 1993, ApJ, 413, L105
Phillips, M. M., Lira, P., Sutzeff, N. B., Schommer, R. A., Hamuy, M., & Maza, J. 1999, AJ, 118, 1766
Phillips, M. M., et al. 2007, PASP, 119, 360,
Pignata, G., et al. 2004, MNRAS, 355, 178
Pignata, G., et al. 2008, MNRAS, 388, 971
Quimby, R., Brown, P., Gerardy, C. 2006b, CBET, 393
Quimby, R., Höflich, P., Kannappan, S. J., Rykoff, E., Rujopakarn, W., Akerlof, C. W., Gerardy, C. L., & Wheeler, J. C. 2006a, ApJ, 636, 400
Rand, R. J. 1995, AJ, 109, 2444
Riess, A. G., et al. 1998, ApJ, 116, 1009
Röpke, F. K., Hillebrandt, W., Schmidt, W., Niemeyer, J. C., Blinnikov, S. I., Mazzali, P. A. 2007, ApJ, 668, 1132
Sahu, D. K., et al. 2008, ApJ, 680, 580
Stanishev, V., et al. 2007, A&A, 469, 645
Suzuki, S., & Migliardi, M. 2006, IAUC, 8667
Tanaka, M., Mazzali, P. A., Maeda, K., Nomoto, K. 2006, ApJ, 645, 470
Tanaka, M., et al. 2008 ApJ, 677, 448
Wang, X., Wang, L., Zhou, X., Lou, Y. Q., & Li, Z. 2005, ApJ, 620L, 87
Wang, X., Wang, L., Pain, R., Zhou, X., & Li, Z. 2006, ApJ, 645, 488
Wang, X., et al. 2008a, ApJ, 675, 626
Wang, X., Li, W., Filippenko, A. V., Foley, R. J., Smith, N., & Wang, L. 2008b, ApJ, 677, 1060

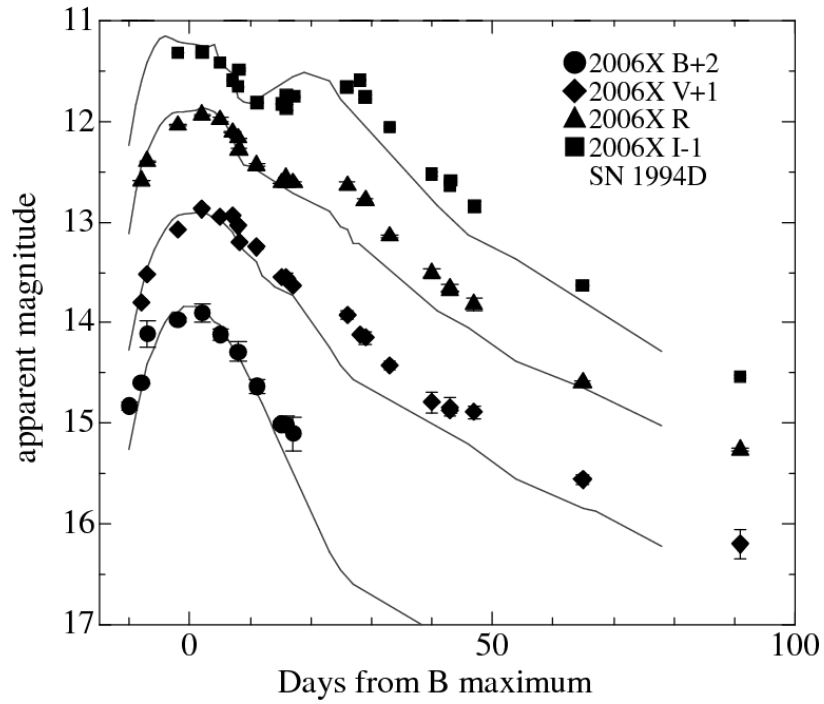


Fig. 1. Light curves of SN 2006X in B , V , Rc and Ic bands (symbols) compared with those of normal SN Ia 1994D (lines, Patat et al. 1996). The extinction in the host and our galaxies has been corrected (see §3.2).

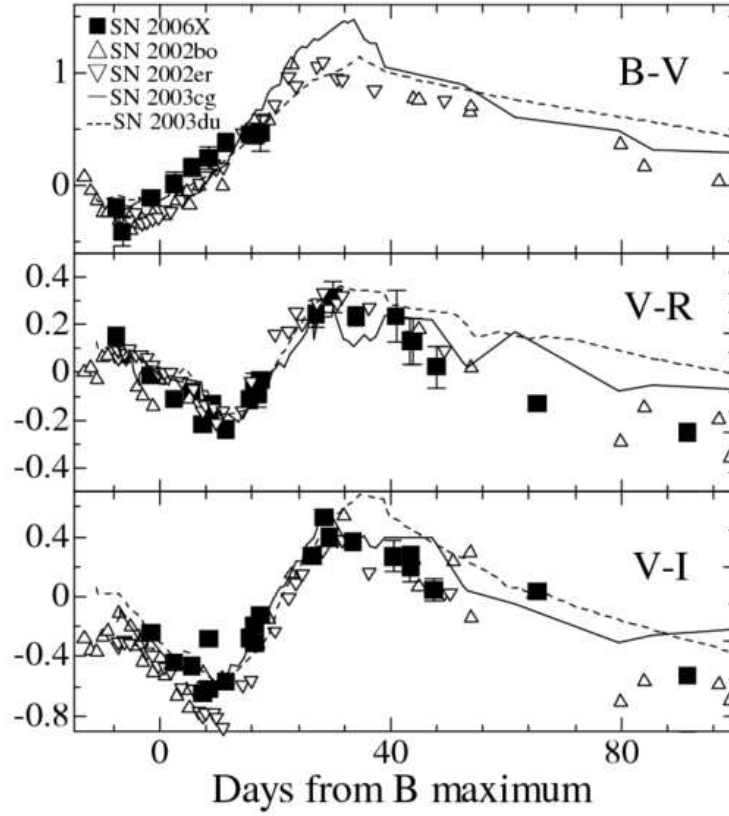


Fig. 2. Reddening-corrected color curves of SN 2006X compared with SNe 2002bo, 2002er, 2003cg and 2003du (Krisciunas et al. 2004; Pignata et al. 2004; Elias-Rosa et al. 2006; Stanishev et al. 2007). The color curves of those comparison SNe are shifted to match the colors of SN 2006X at maximum.

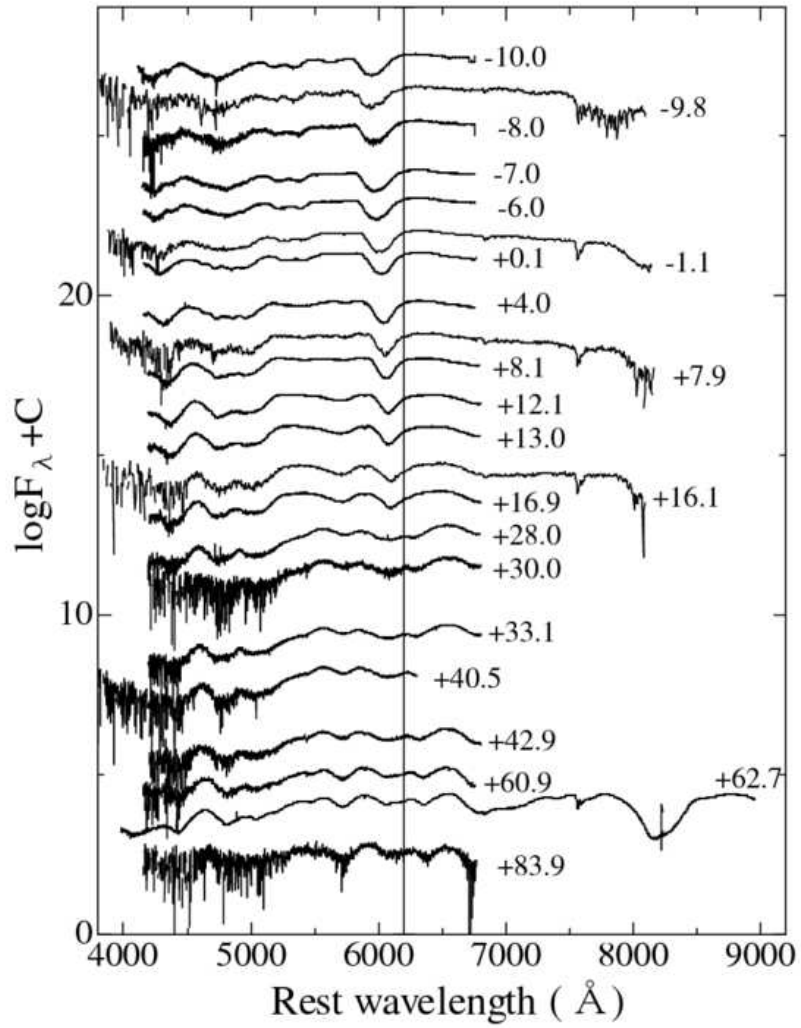


Fig. 3. Spectral evolution of SN 2006X from $t = -10.0$ d to $+83.9$ d. A vertical line is drawn at 6200 \AA to see the evolution of Si II $\lambda 6355$ feature.

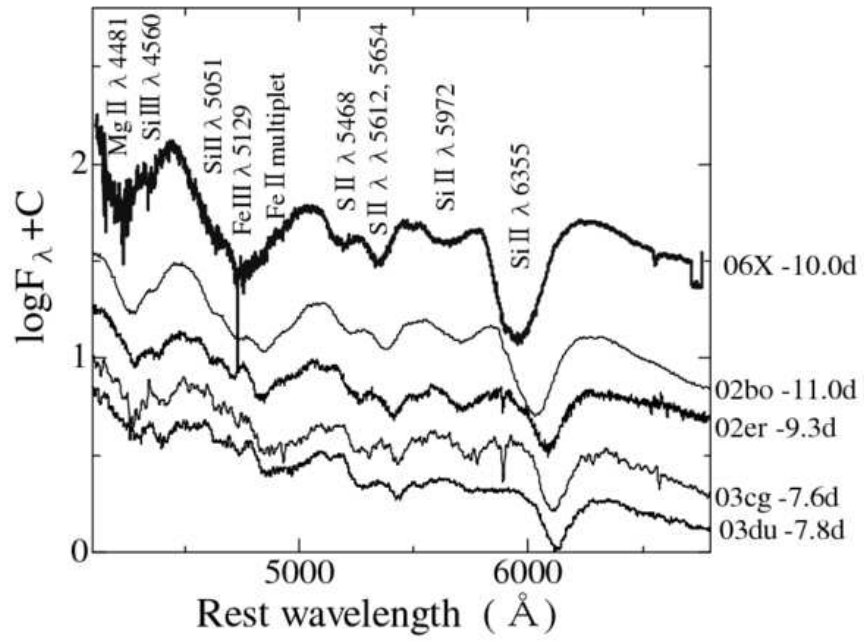


Fig. 4. Spectrum of SN 2006X at $t = -10.0$ d is compared with those of SNe Ia 2002bo, 2002er, 2003cg, and 2003du at similar epochs. The reddening has been corrected.

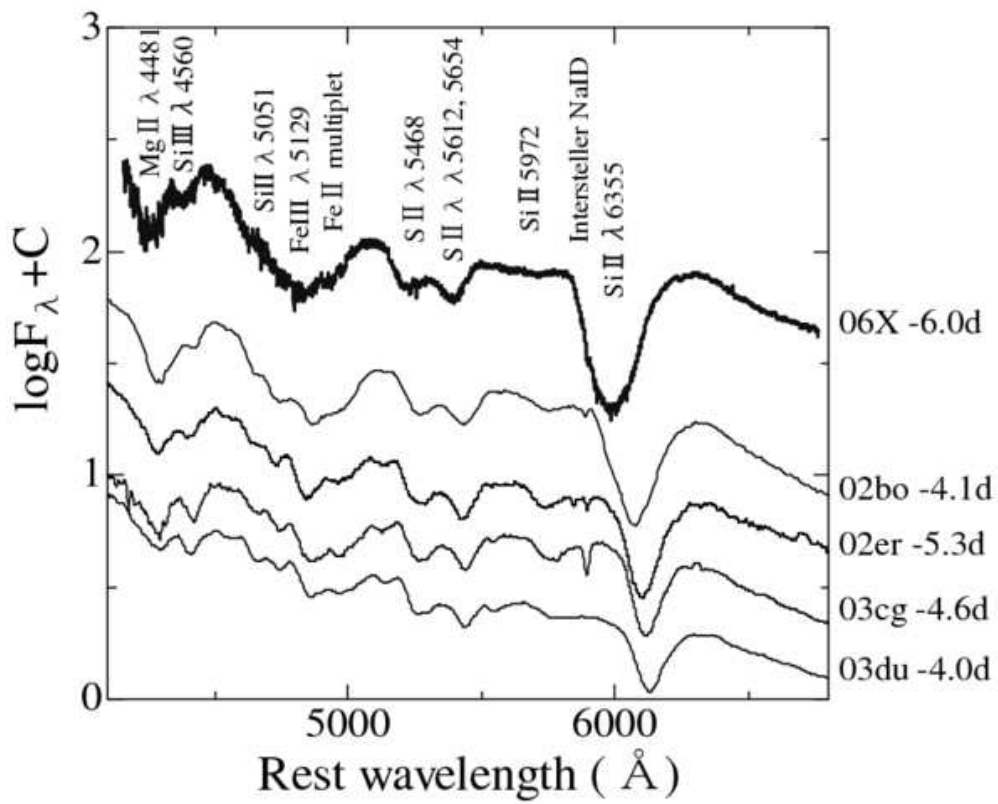


Fig. 5. Same as figure 4, but around $t = -6$ d.

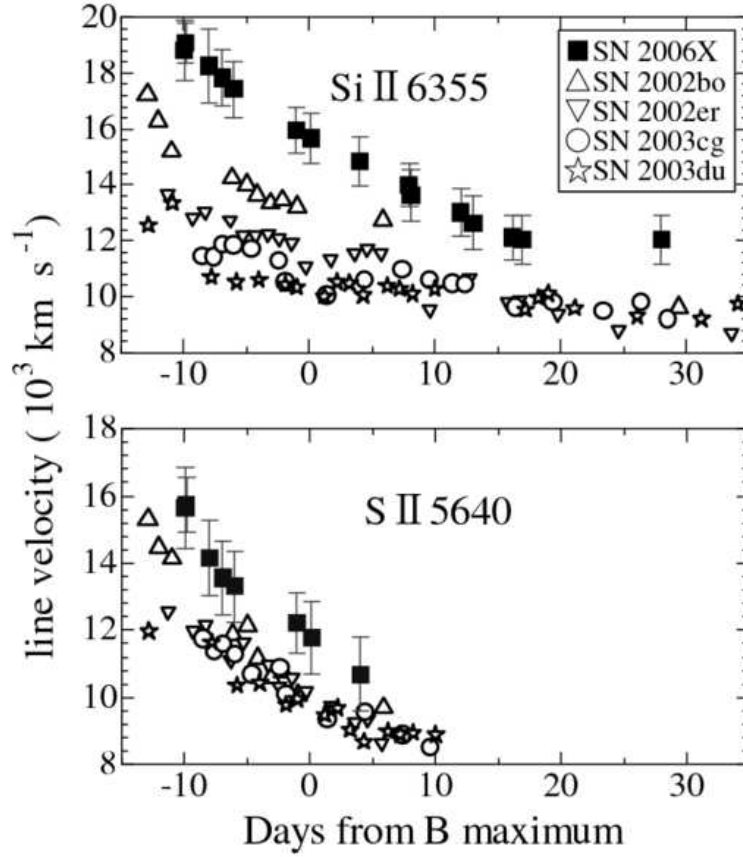


Fig. 6. Time evolution of line velocity of Si II λ 6355 (upper panel) and S II λ 5640 (lower panel). The error bar is estimated by the root sum square of the 1σ error of the velocity measurements by Gaussian fitting and the wavelength resolution of our spectroscopy (see §2.2).

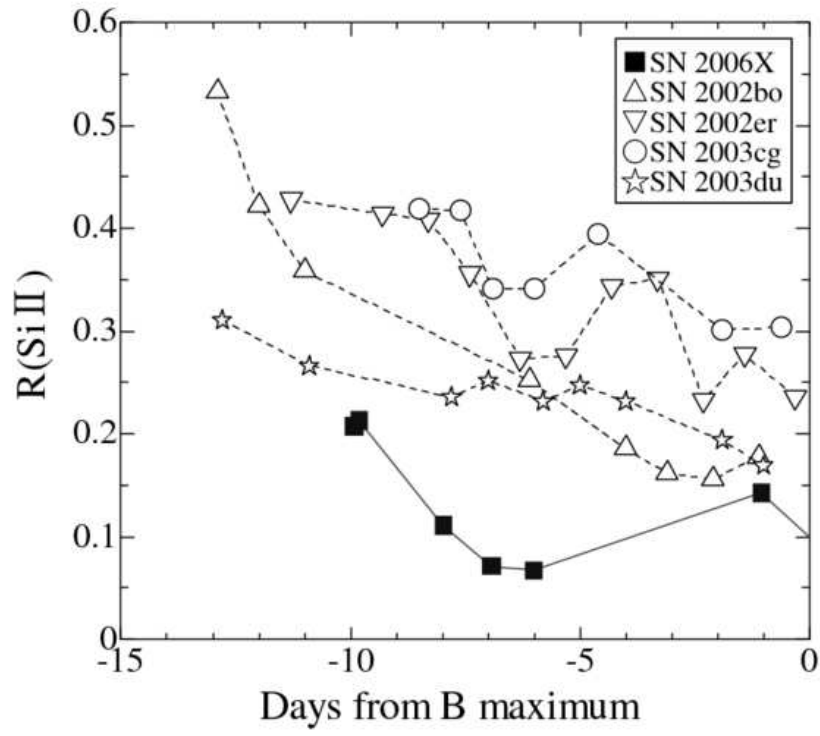


Fig. 7. Time evolution of $\mathcal{R}(\text{Si II})$, the depth ratio of Si II $\lambda 5972$ to Si II $\lambda 6355$, before maximum brightness.

Table 1. The *BVRcIc* photometry for SN 2006X

Date	MJD	Epoch ^a	<i>B</i>	<i>V</i>	<i>Rc</i>	<i>Ic</i>	Obs.
2006/02/09	53775.69	-9.98	16.25 ±0.05				NHAO
2006/02/11	53777.61	-8.06	16.03 ±0.13	14.88 ±0.03	14.09 ±0.02		NHAO
2006/02/12	53778.65	-7.02	15.54 ±0.13	14.61 ±0.01	13.90 ±0.01		NHAO
2006/02/17	53783.61	-2.06	15.39 ±0.02	14.16 ±0.01	13.54 ±0.00	13.17 ±0.01	NHAO
2006/02/21	53787.65	1.98	15.32 ±0.09	13.96 ±0.02	13.44 ±0.00	13.16 ±0.01	NHAO
2006/02/24	53790.66	4.99	15.54 ±0.05	14.04 ±0.01	13.48 ±0.02	13.27 ±0.03	NHAO
2006/02/26	53792.73	7.06		14.03 ±0.01	13.61 ±0.01	13.44 ±0.01	NHAO
2006/02/27	53793.65	7.98	15.71 ±0.09	14.13 ±0.02	13.67 ±0.00	13.51 ±0.01	NHAO
2006/02/27	53793.77	8.10		14.29 ±0.01	13.78 ±0.02	13.34 ±0.01	OKU
2006/03/02	53796.72	11.05	16.06 ±0.08	14.34 ±0.02	13.94 ±0.02	13.67 ±0.01	NHAO
2006/03/06	53800.80	15.13	16.43 ±0.02	14.64 ±0.01	14.11 ±0.00	13.68 ±0.01	NHAO
2006/03/07	53801.56	15.89	16.44 ±0.08	14.64 ±0.04	14.06 ±0.00	13.60 ±0.01	NHAO
2006/03/07	53801.61	15.94		14.65 ±0.05	14.10 ±0.02	13.72 ±0.03	OKU
2006/03/08	53802.76	17.09	16.52 ±0.17	14.72 ±0.01	14.11 ±0.02	13.60 ±0.01	NHAO
2006/03/17	53811.62	25.95		15.02 ±0.04	14.14 ±0.04	13.51 ±0.04	OKU
2006/03/19	53813.81	28.14		15.21 ±0.02		13.44 ±0.00	NHAO
2006/03/20	53814.62	28.95		15.24 ±0.06	14.29 ±0.03	13.61 ±0.02	OKU
2006/03/24	53818.64	32.97		15.52 ±0.04	14.64 ±0.01	13.91 ±0.02	OKU
2006/03/31	53825.61	39.94		15.88 ±0.10	15.01 ±0.04	14.37 ±0.02	OKU
2006/04/03	53828.58	42.91		15.93 ±0.09	15.16 ±0.04	14.49 ±0.04	OKU
2006/04/03	53828.71	43.04		15.96 ±0.04	15.18 ±0.00	14.43 ±0.01	NHAO
2006/04/07	53832.63	46.96		15.98 ±0.06	15.32 ±0.06	14.70 ±0.04	OKU
2006/04/25	53850.54	64.87		16.65 ±0.05	16.10 ±0.01	15.48 ±0.01	NHAO
2006/05/21	53876.62	90.95		17.29 ±0.15	16.76 ±0.02	16.39 ±0.01	NHAO

^a Days measured from the *B*-band maximum, MJD 53785.67

Table 2. Spectroscopic parameters for SN 2006X

Date	MJD	Epoch ^a (days)	Exp. ^b (s)	S II λ 5640 ^c (10^3 km s ⁻¹)	Si II λ 6355 ^c (10^3 km s ⁻¹)	$\mathcal{R}(\text{Si II})$	Obs.
2006/02/09	53775.71	-9.96	5400	15.6 ± 1.2	18.8 ± 1.1	0.207 ± 0.012	NHAO
2006/02/09	53775.81	-9.86	540	15.7 ± 0.8	19.1 ± 0.7	0.213 ± 0.024	GAO
2006/02/11	53777.65	-8.02	1800	14.2 ± 1.1	18.3 ± 1.3	0.111 ± 0.026	NHAO
2006/02/12	53778.71	-6.96	3600	13.6 ± 1.1	17.8 ± 1.0	0.071 ± 0.016	NHAO
2006/02/13	53779.63	-6.04	3600	13.3 ± 1.1	17.4 ± 1.0	0.068 ± 0.011	NHAO
2006/02/18	53784.59	-1.08	900	12.2 ± 0.9	16.0 ± 0.8	0.143 ± 0.024	GAO
2006/02/19	53785.77	0.10	3600	11.8 ± 1.1	15.7 ± 0.9	0.093 ± 0.007	NHAO
2006/02/23	53789.65	3.98	3600	10.7 ± 1.1	14.9 ± 0.9		NHAO
2006/02/27	53793.58	7.91	1500		14.0 ± 0.8		GAO
2006/02/27	53793.74	8.07	1800		13.6 ± 0.9		NHAO
2006/03/03	53797.71	12.04	3600		13.0 ± 0.8		NHAO
2006/03/04	53798.65	12.98	1800		12.6 ± 1.0		NHAO
2006/03/07	53801.80	16.13	900		12.1 ± 0.8		GAO
2006/03/08	53802.60	16.93	3600		12.0 ± 0.9		NHAO
2006/03/19	53813.64	27.97	3600		12.0 ± 0.9		NHAO
2006/03/21	53815.67	30.00	3600				NHAO
2006/03/24	53818.73	33.06	3600				NHAO
2006/03/31	53826.11	40.44	3600				NHAO
2006/04/03	53828.53	42.86	3600				NHAO
2006/04/21	53846.55	60.88	3600				NHAO
2006/04/23	53848.34	62.67	1200				Subaru
2006/05/14	53869.57	83.90	7200				NHAO

^a Days measured from the *B*-band maximum. ^b Total exposure time. ^c Line velocity measured at the line center (see §2.2)